RAPID COMMUNICATIONS

PHYSICAL REVIEW B VOLUME 52, NUMBER 14 1 OCTOBER 1995-II

Low-temperature structural behavior of Sr_2RuO_4

T. Vogt
Department of Physics, Brookhaven National Laboratory, Upton, New York 11973

D. J. Buttrey
Department of Chemical Engineering, University of Delaware, Newark, Delaware 19716

(Received 23 June 1995)

Using high-resolution neutron powder diffraction we have shown that in Sr_2RuO_4 the onset of superconductivity is not accompanied by long-range structural distortions. This is in marked contrast to the isostructural copper-containing layered perovskites and points toward a more conventional superconducting mechanism. We have observed a structural response to the metal-to-insulator phase transition near 100 K.

The recent discovery of superconductivity in Sr_2RuO_4 ($T_c = 0.93$ K) (Ref. 1) provides clear evidence of superconducting behavior in a noncuprate oxide with the K_2NiF_4 structure. Understanding the relationship between this ruthenate and the high-T_c family of cuprates might point toward the peculiarities of the latter. It is of particular interest that in Sr_2RuO_4 a second-row transition metal is in the B site and that the spin state is $S=1$ (low spin, $4d^4$), as opposed to the $S=1/2$ ($3d^9$) in the cuprates. Examining these differences in the electronic structure of isostructural compounds might address the question why copper is so special with regard to superconductivity.

Across the first-row transition metal series, initially the high-spin ions show a decrease in ionic radius for a given valence, which is due to changes in the crystal-field stabilization and the increased nuclear charge Z. As the high energy e_g orbitals are being populated, their antibonding character leads to a reversal of this trend and longer metal-to-oxygen distances are the result. The second- and third-row transition metals are generally low spin ions and no interruption of the ionic radius contraction is observed.

For further comparison, the first-row $S=1$ Ni^{2+} (high spin, $3d^8$) layered perovskites appear not to be superconducting, nor does the second-row $S=1/2$ rhodium analog (low-spin, $4d^5$) Sr_2RhO_4.[1] Another interesting difference between the first- and second-row transition metal containing compounds is the defect accommodation. Oxides of the type Ln_2MO_4 with the K_2NiF_4 structure containing first-row transition metals such as $M=Co^{2+}$, Ni^{2+}, Cu^{2+} are readily hole doped via intercalation of excess oxygen or by heterovalent substitution on the A site (e.g., by Sr^{2+} or Ba^{2+} for Ln^{3+}). In the case of Ru^{4+} the electroneutrality of the Sr_2O_2 rock-salt layer does not encourage the intercalation of excess oxygen. Thus the cuprates are insulating unless they are hole doped, whereas the ruthenate is intrinsically a poor metal or superconductor. In the cuprates, electronic states at the Fermi level are induced by hole doping; in the ruthenates, these states arise as a result of decreased electron correlations. Unfortunately, in the case of the ruthenate it seems that T_c is in the vicinity of 1 K, 20–50 times lower than the corresponding doped K_2NiF_4-type cuprates.

In the case of $La_{2-x}Ba_xCuO_4$ the resistivity is strongly influenced by low-temperature structural phase transitions. According to Maeno *et al.*,[1] x-ray investigations of the low-temperature structure of Sr_2RuO_4 down to 5 K did not show any evidence of structural changes. Detailed structural data near T_c (~ 1 K) are therefore highly desirable to establish

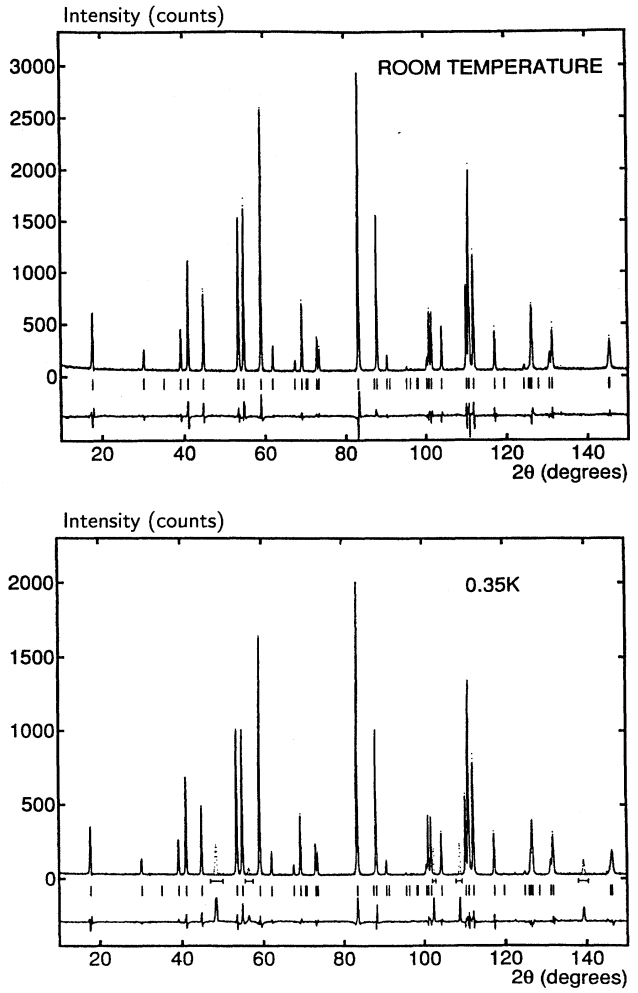

FIG. 1. Rietveld refinement plots of Sr_2RuO_4 at room temperature and 0.35 K. For details see text.

TABLE I. Crystallographic parameters of Sr_2RuO_4 at various temperatures refined in the space group $I4/mmm$ (No. 139, International Tables for Crystallography).

Temperature		a		c			
295 K	3.87100(9)			12.7397(4)			
		x	y	z	$B(1,1)$	$B(2,2)$	$B(3,3)$
	Sr	0	0	0.3526(3)	0.6(1)	0.6(1)	0.5(2)
	Ru	0	0	0	0.2(1)	0.2(1)	0.9(3)
	O(1)	1/2	0	0	0.5(2)	0.4(2)	1.0(2)
	O(2)	0	0	0.1620(4)	0.7(1)	0.7(1)	0.4(3)
200 K	3.86656(8)			12.7323(3)			
	Sr	0	0	0.3525(3)	0.5(1)	0.5(1)	0.2(2)
	Ru	0	0	0	0.1(1)	0.1(1)	0.3(2)
	O(1)	1/2	0	0	0.1(2)	0.0(2)	0.8(2)
	O(2)	0	0	0.1615(4)	0.6(1)	0.6(1)	0.3(2)
150 K	3.8644(1)			12.7256(5)			
	Sr	0	0	0.3521(4)	0.4(1)	0.4(1)	0.4(3)
	Ru	0	0	0	0.3(2)	0.3(2)	0.0(3)
	O(1)	1/2	0	0	0.0(2)	0.7(2)	0.1(2)
	O(2)	0	0	0.1633(4)	0.4(1)	0.4(1)	0.1(3)
100 K	3.8630(1)			12.7240(4)			
	Sr	0	0	0.3524(3)	0.4(1)	0.4(1)	0.7(2)
	Ru	0	0	0	0.1(1)	0.1(1)	0.7(2)
	O(1)	1/2	0	0	0.0(2)	0.6(2)	0.1(2)
	O(2)	0	0	0.1635(3)	0.5(1)	0.5(1)	0.2(3)
50 K	3.86229(9)			12.7229(4)			
	Sr	0	0	0.3527(3)	0.3(1)	0.3(1)	0.4(2)
	Ru	0	0	0	0.2(1)	0.2(1)	0.3(3)
	O(1)	1/2	0	0	0.2(2)	0.2(2)	0.4(2)
	O(2)	0	0	0.1619(4)	0.4(1)	0.4(1)	0.3(3)
12 K	3.86122(9)			12.7214(4)			
	Sr	0	0	0.3526(4)	0.3(1)	0.3(1)	0.6(2)
	Ru	0	0	0	0.0(1)	0.0(1)	0.6(3)
	O(1)	1/2	0	0	0.0(2)	0.5(2)	0.1(2)
	O(2)	0	0	0.1633(4)	0.4(1)	0.4(1)	0.1(3)
8 K	3.86132(8)			12.7218(4)			
	Sr	0	0	0.3529(4)	0.3(1)	0.3(1)	0.6(2)
	Ru	0	0	0	0.0(1)	0.0(1)	0.6(3)
	O(1)	1/2	0	0	0.0(2)	0.8(2)	0.0(2)
	O(2)	0	0	0.1634(4)	0.5(1)	0.5(1)	0.1(3)
6 K	3.86145(7)			12.7220(3)			
	Sr	0	0	0.3526(3)	0.3(1)	0.3(1)	0.6(2)
	Ru	0	0	0	0.0(1)	0.0(1)	0.5(3)
	O(1)	1/2	0	0	0.0(2)	0.7(2)	0.1(2)
	O(2)	0	0	0.1633(4)	0.4(1)	0.4(1)	0.1(3)
4.4 K	3.86135(7)			12.7216(3)			
	Sr	0	0	0.3524(3)	0.4(1)	0.4(1)	0.7(2)
	Ru	0	0	0	0.1(1)	0.1(1)	0.7(2)
	O(1)	1/2	0	0	0.0(2)	0.6(2)	0.1(2)
	O(2)	0	0	0.1635(3)	0.5(1)	0.5(1)	0.2(3)
0.35 K	3.86111(7)			12.7217(3)			
	Sr	0	0	0.3533(3)	0.1(1)	0.1(1)	0.5(2)
	Ru	0	0	0	0.0(1)	0.0(1)	0.4(2)
	O(1)	1/2	0	0	0.0(2)	0.7(2)	0.2(2)
	O(2)	0	0	0.1628(3)	0.4(1)	0.4(1)	0.0(2)

similarities or differences with copper-containing layered perovskites. Sr_2RuO_4 shows a pronounced anisotropy of the normal-state resistivity: The resistivity in the RuO_2 plane ρ_{ab} is $\sim 10^{-4}$ Ω cm perpendicular to it $\rho_c \sim 4\times 10^{-2}$ Ω cm. The electronic anisotropy characterized by the ratio of ρ_c/ρ_{ab} is ~ 220 at room temperature and increases to ~ 850 at 2 K. Near $T \sim 130$ K ρ_c exhibits a crossover from nonmetallic to metallic behavior.[1] A careful search for a small structural variation associated with the metal-to-insulator transition would provide valuable insights into its origin which is thought to be purely electronic.

We performed low-temperature neutron powder diffraction measurements below and above T_c using the high-resolution neutron powder diffractometer at the High Flux Beam Reactor at Brookhaven National Laboratory. The instrument offers a resolution of $\Delta d/d \sim 5\times 10^{-4}$ at a wavelength of 1.8857 Å. The unique design of the vertically focusing monochromator is based on using Ge(115) wafer stacks[2,3] where each wafer was deformed to obtain the desired anisotropic mosaic and then reassembled to 24 stacks. These were independently focused onto the sample position to provide a symmetrical peak profile at an optimized resolution and flux. The detector array is made out of 64 ^{3}He detectors separated by 2.5° in 2θ.

The data were refined using PROFIL, a Rietveld refinement program written by J. K. Cockcroft (University of Birbeck, U.K.). Refined crystallographic parameters are provided in Table I. The room temperature parameters agree well with those of a single crystal x-ray study published by Walz and Lichtenberg[4] as well as with the results of Rietveld refinements of neutron powder diffraction pattern by Huang *et al.*[5] and Neumeier *et al.*[6] The low-temperature structural data are also similar to the data at 13 and 10 K presented by Huang *et al.*[5] and Neumeier *et al.*,[6] respectively.

On cooling no change in the symmetry of the unit cell could be detected. Two neutron powder diffraction patterns

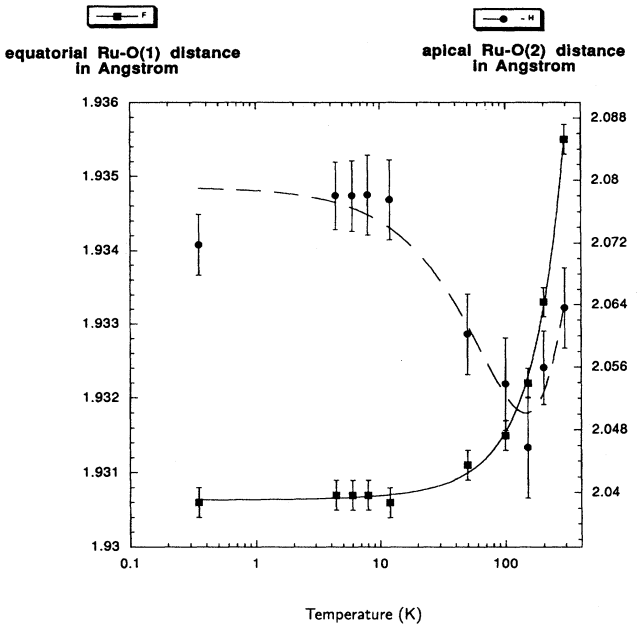

FIG. 2. The variation of the equatorial and axial Ru-O distances in the RuO_6 octahedra of Sr_2RuO_4 as a function of temperature. The ratio of these two distances is a measure of the D_{4h} distortion.

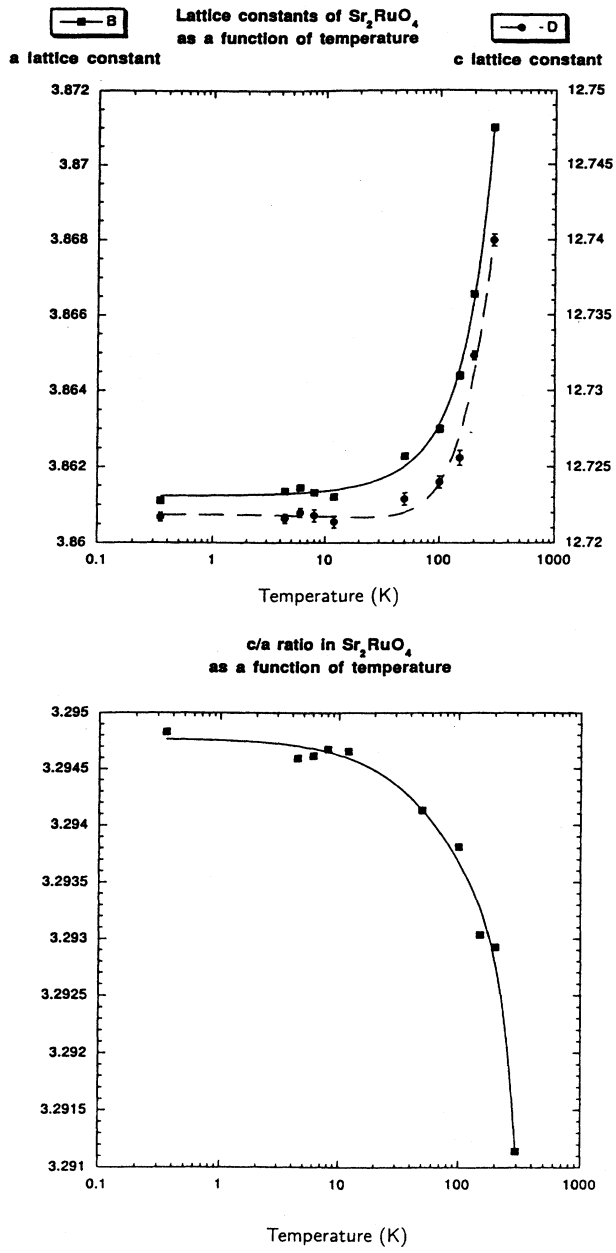

FIG. 3. The variation of the lattice constants and the c/a ratio of Sr_2RuO_4 as a function of temperature.

are presented in Fig. 1, one at room temperature and the second at $T=0.35$ K. The extra peaks present in the 0.35 K are due to the aluminum heat shields in the $^3He/^4He$ cryostat. The tick marks indicate the positions of the allowed Bragg reflections in space group $I4/mmm$; the lower curve is the difference between observed and refined intensities.

It is apparent from the results presented in Table I that the a lattice constant contracts by roughly twice as much as c when cooling down to 0.35 K. This leads to an anisotropic squashing of the RuO_6 octahedra: the four equatorial Ru-O(1) are shortened as the apical Ru-O(2) are elongated by the same amount as the shortest Sr-O(2) distance is reduced. The net result is a tighter octahedral packing and an increased tetragonal distortion of the RuO_6 octahedra. This D_{4h} distortion of the octahedra can be accompanied by tilting at low temperatures, as is the case in other layered perovskites structures such as $La_{2-x}Sr_xCuO_4$. It has been shown that some phase transitions due to octahedral tilts are continuous so that the resulting low-temperature structure can be determined by irreducible representations of the high-temperature space group. The librational phonon modes involved transform accordingly and correspond in many cases to soft modes that condense at the phase transition. In the case of Sr_2RuO_4!, the D_{4h} distortion is enhanced when cooling and no first-order structural phase transition is observed. There is a clear enhancement of the D_{4h} distortion around 100 K. Figure 2 shows that while the equatorial Ru-O(1) distance continues to decrease and then levels off near 10 K, the apical Ru-O(2) distance increases after the transition into the metallic state. In a simple angular overlap model the D_{4h} distortion of the RuO_6 octahedra causes the low-lying t_{2g} orbitals to be split into two groups. Increasing the tetragonal distortion when cooling by elongating the apical Ru-O(2) distance will perturb the d_{xz} and d_{yz} orbital more than the d_{xy} orbital. The ratio of the two ruthenium-to-oxygen distances in the RuO_6 octahedra is a crude approximation of the energetic difference of the two t_{2g} levels created by the D_{4h} distortion. This can lead to an effective charge transfer from the d_{xz} and d_{yz} levels into the d_{xy} level. Cava *et al.*[7] have investigated the insulator-to-metal transition in $Sr_2Ir_{1-x}Ru_xO_4$ solid solutions and found that the ratio of the lattice parameters c/a increases with increasing Ir concentra-

tion. At an Ir concentration of roughly 0.3 ($x=0.7$) there is a noticeable change in slope. This critical concentration coincides with a maximum in the Curie moment per formula unit. Above 70% Ru concentration the local moment falls off dramatically and in pure Sr_2RuO_4 virtually no localized moments are left. Thus the increase of the c/a ratio in Sr_2RuO_4 (Fig. 3) on cooling appears to mimic this behavior and can be associated with a transition from a localized to itinerant electronic state near 100 K.

This research was supported by the Division of Materials Sciences, U.S. Department of Energy, under Contract No. DE-AC02-76CH00016.

[1] Y. Maeno, H. Hashimoto, K. Yoshida, S. Nishizaki, T. Fujita, J. G. Bednorz, and F. Lichtenberg, Nature (London) **372**, 532 (1994).

[2] T. Vogt, L. Passell, S. Cheung, and J. D. Axe, Nucl. Instrum. Methods A **338**, 71 (1994).

[3] J. D. Axe, S. Cheung, D. E. Cox, L. Passell, and T. Vogt, Neutron News **2** (3), 85 (1994).

[4] L. Walz and F. Lichtenberg, Acta Crystallogr. Sect. C **49**, 1268 (1993).

[5] Q. Huang, J. L. Soubeyroux, O. Chmaissem, I. Natali Sora, A. Santoro, R. J. Cava, J. J. Krajewski, and W. F. Peck, Jr., J. Solid State Chem. **112**, 355 (1994).

[6] J. J. Neumeier, M. F. Hundley, M. G. Smith, J. D. Thompson, C. Allgeier, H. Xie, W. Yelon, and J. S. Kim, Phys. Rev. B **50**, 17 910 (1994).

[7] R. J. Cava, B. Batlogg, K. Kiyono, H. Takagi, J. J. Krajewski, W. F. Peck, Jr., L. W. Rupp, Jr., and C. H. Chen, Phys. Rev. B **49**, 11 890 (1994).